BIOCHEMISTRY

© Copyright 2006 by the American Chemical Society Volume 45, Number 15 April 18, 2006

Accelerated Publications

Hydration and Packing along the Folding Pathway of SH3 Domains by Pressure-Dependent NMR†

Irina Bezsonova,[‡,§] Dmitry M. Korzhnev,[‡,||,⊥] R. Scott Prosser,[‡] Julie D. Forman-Kay,[§,||] and Lewis E. Kay*[,‡,||,⊥]

Department of Chemistry, University of Toronto, Toronto, Ontario, Canada M5S 3H6, The Hospital for Sick Children, Toronto, Ontario, Canada M5G 1X8, Department of Biochemistry, University of Toronto, Toronto, Ontario, Canada M5S 1A8, and Department of Medical Genetics, University of Toronto, Toronto, Ontario, Canada M5S 1A8

Received January 26, 2006; Revised Manuscript Received March 3, 2006

ABSTRACT: The volumetric properties associated with protein folding transitions reflect changes in protein packing and hydration of the states that participate in the folding reaction. Here, NMR spin relaxation techniques are employed to probe the folding−unfolding kinetics of two SH3 domains as a function of pressure so that the changes in partial molar volumes along the folding pathway can be measured. The two domains fold with rates that differ by ∼3 orders of magnitude, so their folding dynamics must be probed using different NMR relaxation experiments. In the case of the drkN SH3 domain that folds via a two-state mechanism on a time scale of seconds, nitrogen magnetization exchange spectroscopy is employed, while for the G48M mutant of the Fyn SH3 domain where the folding occurs on the millisecond time scale (three-step reaction), relaxation dispersion experiments are utilized. The NMR methodology is extremely sensitive to even small changes in equilibrium and rate constants, so reliable estimates of partial molar volumes can be obtained using low pressures (1−120 bar), thus minimizing perturbations to any of the states along the folding reaction coordinate. The volumetric data that were obtained are consistent with a similar folding mechanism for both SH3 domains, involving early chain compaction to states that are at least partially hydrated. This work emphasizes the role of NMR spin relaxation in studying dynamic processes over a wide range of time scales.

A description of the structural and thermodynamic properties of the states that are produced during the protein folding reaction is critical for understanding the process(es) by which proteins fold and for obtaining insight into the folding energy landscape (*1*, *2*). Structural information about the folded state end point is often readily obtained by X-ray diffraction and/or NMR spectroscopy, while studies of the unfolded ensemble can be performed using a variety of different spectroscopic approaches (*1*), with NMR playing a very prominent role (*3*, *4*). Detailed information about intermediates and transitions state ensembles (TSEs) is more difficult to obtain because such states are generally populated at low levels and not readily isolated. As a result, they are often studied indirectly, by introducing mutations or by invoking changes in variables such as temperature, pressure, solvent conditions, or denaturant concentration (*1*, *5*).

† This work was supported by grants from the Natural Sciences and Engineering Research Council of Canada (NSERC) to L.E.K. and R.S.P. and by the Canadian Institutes of Health Research (CIHR) to L.E.K. and J.D.F.-K. I.B. is the recipient of a Ph.D. fellowship form the CIHR Training Program in Protein Folding. D.M.K. acknowledges support in the form of a CIHR postdoctoral fellowship. L.E.K. holds a Canada Research Chair in Biochemistry.

* To whom correspondence should be addressed. Phone: (416) 978-0741. Fax: (416) 978-6885. E-mail: kay@pound.med.utoronto.ca.

‡ Department of Chemistry, University of Toronto.

§ The Hospital for Sick Children.

|| Department of Biochemistry, University of Toronto.

⊥ Department of Medical Genetics, University of Toronto.

10.1021/bi060177r CCC: $33.50 © 2006 American Chemical Society
Published on Web 03/22/2006

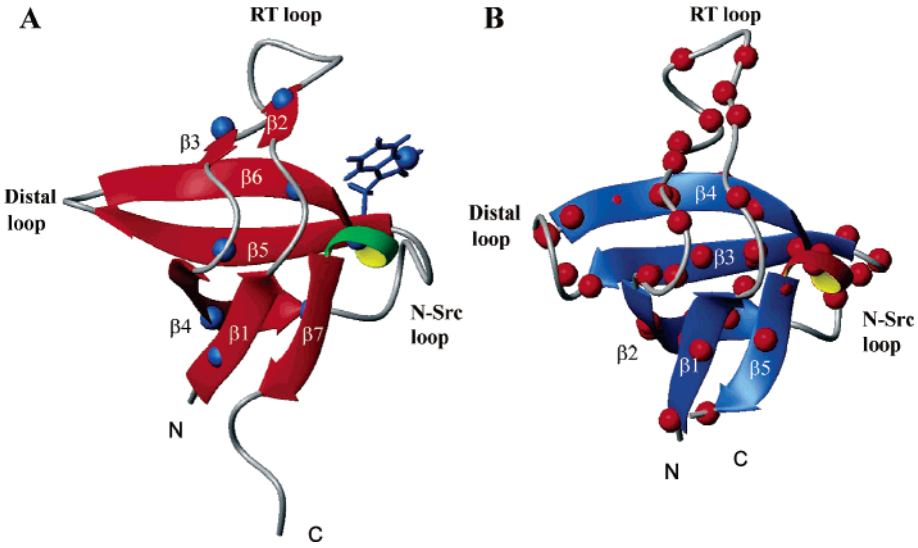

FIGURE 1: Ribbon diagrams of the backbone structures of the (A) drkN (*22*) and (B) Fyn SH3 (*48*) domains (PDB entries 2A36 and 1ZBJ, respectively). The locations of the ^{15}N probes of exchange are indicated.

In principle, volumetric parameters such as partial molar volumes and compressibilities can provide important information about both structural and hydration properties of transient, weakly populated states along the folding trajectory (*6*−*8*). These parameters have been the subject of both theoretical and experimental studies, with characteristic differences observed between folded (F), unfolded (U), partially folded, and molten-globule states (*6*, *7*). Traditionally, changes in volumetric properties between F and U have been derived from density and sound velocity measurements performed at atmospheric pressure as a function of denaturant (*6*, *9*), or from experiments where high pressure (often several thousand bars) is employed as the perturbant (*10*−*12*), while volumetric properties of the TSE have been studied by pressure-jump or stopped-flow kinetic experiments performed under high pressure (*13*). Interpretation of data from such experiments is, however, not without complication. For example, in experiments performed as a function of denaturant, F and U states are probed under very different conditions (for example, the F state at neutral pH or zero guanidinium concentration and the U state at low pH or high guanidinium concentration) and subtle changes in the structure of the U ensemble as a function of denaturant can affect measured volume changes associated with folding (*14*). Similarly, high pressures can also lead to changes in structural properties of U, TSE, or intermediates.

In this study, we use NMR spectroscopy as a very sensitive tool to probe the folding kinetics of two Src homology 3 (SH3) domains as a function of pressure, from which changes in partial molar volumes can be obtained. The SH3 domains that were chosen fold with rates that differ by ~3 orders of magnitude, so different NMR methods must be used to study the kinetics for each system. The N-terminal SH3 domain of the *Drosophila* adapter protein Drk (drkN SH3), shown in Figure 1A, interconverts between highly populated F and U states in aqueous buffer via a two-state mechanism with exchange rates that are slow on the NMR chemical shift time scale, so separate sets of peaks are observed for each state (*15*, *16*). In what follows, we refer to these U and F states as U_{exch} and F_{exch}, respectively, to emphasize the equilibrium between approximately equally populated folded and unfolded conformers under nondenaturing conditions and to distinguish these states from those that exist under denaturing or salt-stabilizing conditions, consistent with previous publications (*15*). The pressure dependence of folding and unfolding rates for the drkN SH3 domain has been measured via longitudinal exchange NMR spectroscopy (*17*) that has been used previously to probe electrostatic interactions in the folding transition state of this protein (*18*) and recently to study folding kinetics as a function of urea and glycerol (M. Tollinger et al., manuscript in preparation). The second protein, a G48M mutant SH3 domain from the Fyn tyrosine kinase (G48M Fyn SH3), shown in Figure 1B, folds on a millisecond time scale through an intermediate, I (*19*, *20*). In this case, both U and I states are only transiently populated (approximately 5 and 1% for U and I, respectively, for a perdeuterated protein, at 25 °C) so that peaks are not observed in NMR spectra for these states. Folding kinetics of the G48M Fyn SH3 domain can be studied by Carr−Purcell−Meiboom−Gill (CPMG) relaxation dispersion techniques (*21*). As we will show, the exquisite sensitivity of the methodologies used to quantify folding−unfolding rates in both systems allows very low pressures (≤120 bar) to be used, minimizing any subtle changes in structures of the U or I state ensembles that might otherwise result. Despite the fact that the exchange dynamics of drkN and G48M Fyn SH3 domains are interpreted using different models (two- vs three-site exchange) and that substantial differences in the time scales of folding are noted, the volume profiles along the folding pathway are remarkably similar for both proteins, consistent with an initial collapse to states that are at least partially hydrated.

MATERIALS AND METHODS

Probing Folding of the drkN SH3 Domain. The folding−unfolding kinetics of the drkN SH3 domain have been studied using the nitrogen longitudinal exchange experiment described by Farrow et al. (*17*) and analyzed using the procedure discussed by Tollinger and co-workers (*16*). The interested reader is referred to the literature for details of the experiment, as well as for the equations that were used to fit the magnetization exchange profiles.

Magnetization exchange experiments were performed on ^{15}N-labeled samples of the drkN SH3 domain, 0.8 mM in

protein, with 50 mM sodium phosphate and 10% D_2O at pH 6 and 15 °C on a Varian *Inova* spectrometer operating at 500 MHz (^{1}H frequency) and equipped with a room-temperature triple-resonance probe head. Samples were prepared as described previously (*22*). Experiments were carried out using a sapphire tube (Saint-Gobain Crystals, Milford, NH) with a 3.0 mm inner diameter at six pressures (using nitrogen gas to pressurize), ranging from 1 to 75 bar (1, 15, 30, 45, 60, and 75 bar). Each sample was used for exchange measurements at two pressures over a period of no longer than 2 days. No evidence of any irreversible process such as aggregation that would lead to changes in the ratios of intensities of F and U correlations was observed. At each pressure, a series of 8−11 two-dimensional (2D) ^{1}H−^{15}N exchange spectra was recorded with mixing times (T) ranging from 0 to 560 ms.

Volumes of auto-peaks and cross-peaks in exchange spectra were quantified using the MUNIN approach (*23*, *24*), as described in the Supporting Information. Exchange data were analyzed for nine residues with nonoverlapped auto-peaks and exchange cross-peaks, one pressure point at a time. Residues Ala 3, Ser 10, Ser 18, Thr 22, Ile 27, Met 30, Trp 36 (side chain), Ile 48, and Tyr 52 were included in the analysis and are distributed throughout the protein as indicated in Figure 1A. For these residues, the volumes of both auto-peaks and cross-peaks were fit simultaneously using equations that describe the time evolution of nitrogen magnetization due to exchange (*16*) with folding and unfolding rate constants, k_f and k_u, considered to be the same for all residues (i.e., treated as global parameters). Intrinsic longitudinal relaxation rates were included in the fit for each residue in both folded and unfolded states. Uncertainties in the extracted model parameters (including k_f and k_u) were estimated using the covariance matrix method (*25*). Values of k_f, k_u, and K_{eq} ($=k_u/k_f$) obtained from independent fits of exchange data at each of the six pressures were than fit to the following set of equations

$$k_f = (k_B\kappa T/h)\exp[-\Delta G_{TS-U}/(RT)]$$

$$k_u = (k_B\kappa T/h)\exp[-\Delta G_{TS-F}/(RT)]$$

$$K_{eq} = k_u/k_f = \exp[-\Delta G_{U-F}/(RT)] \quad (1)$$

where k_B is Boltzmann's constant, h is Planck's constant, T is the temperature, R is the universal gas constant, κ is a transmission coefficient, and ΔG_{TS-U}, ΔG_{TS-F}, and ΔG_{U-F} are free energy differences between TS (transition state) and U_{exch}, TS and F_{exch}, and U_{exch} and F_{exch} states, respectively. The pressure dependence of the free energy differences is in turn expressed by the equation $\Delta G_{i-j} = \Delta G_{0,i-j} + \Delta V_{i-j}(P - P_0)$ (i, j $\in$ {TS, F_{exch}, U_{exch}}), where $\Delta G_{0,i-j}$ denotes the folding free energy difference at P_0 (1 bar) and ΔV_{i-j} is the difference in partial molar volumes between states i and j. A κ value of 1.6×10^{-7} has been used as an empirical estimate for protein folding reactions (*26*), corresponding to a $k_B\kappa/h$ of 3000 s^{-1} K^{-1}. *F*-Test statistical analyses show that there are significant improvements to fits of the pressure dependencies of both k_f and K_{eq} when a model in which $\Delta V_{i-j} \neq 0$ is used (relative to one in which $\Delta V_{i-j} = 0$; $p \sim 10^{-5}$), although further improvements in fits with more complex models are not obtained. The uncertainties of the extracted parameters (i.e., ΔV_{i-j} and k_0, where k_0 denotes the equilibrium rate constants at 1 bar) were estimated using the covariance matrix method (*25*).

Probing Folding of the G48M Fyn SH3 Domain. The folding reaction of the [^{2}H,^{15}N]G48M Fyn SH3 domain at 25 °C has been studied in detail previously using a suite of six CPMG-type relaxation dispersion experiments that have been designed for the characterization of millisecond time scale conformational exchange (*20*). Analysis of data from the six types of experiments has shown that the folding reaction can be described in terms of exchange among folded (F), intermediate (I), and unfolded (U) states (F ↔ I ↔ U). In this work, we have used a reduced set of dispersion experiments (^{15}N and ^{1}H single-quantum CPMG data sets) measured at a single magnetic field strength as a function of pressure to extract volumetric parameters. A limited data set has been employed so that the pressure studies could be completed in reasonable measuring times to ensure sample integrity. The data sets have been analyzed using previously determined ^{15}N and ^{1}H chemical shift differences (parts per million) among the exchanging states ($\Delta\varpi_{N,FU}$, $\Delta\varpi_{N,FI}$, $\Delta\varpi_{H,FU}$, and $\Delta\varpi_{H,FI}$) that are robust as they have been measured from a full set of six dispersion profiles recorded on a perdeuterated Fyn SH3 domain sample at fields of 11.7, 14.1, and 18.8 T, and at a pressure of 1 bar, at 25 °C (*20*). In this regard, shift differences very similar to those obtained in that study were extracted from an analysis of dispersion data measured on a methyl-protonated, highly deuterated sample of the Fyn SH3 domain (*27*). Although chemical shift changes with pressure cannot be ruled out, such effects are likely to be very small at the pressures used here ($\leq$120 bar); in the case of a pressure study involving a mutant of apocytochrome b_{562} using ^{15}N relaxation dispersion NMR, $\partial\Delta\varpi_N/\partial P = 0.00067$ ppm/bar, corresponding to differences in $\Delta\varpi_N$ values of less than 0.1 ppm between pressures of 1 and 120 bar (*28*).

^{15}N (*16*, *29*) and ^{1}H (*30*) single-quantum CPMG dispersion profiles were recorded on a [^{2}H,^{15}N]G48M Fyn SH3 sample [1.0 mM protein, 50 mM sodium phosphate, 0.2 mM EDTA, 0.05% NaN_3, and 5% D_2O (pH 7)], prepared as described previously (*19*), using pulse schemes and experimental parameters that have been discussed in the literature (*20*). A sapphire NMR tube (Saint-Gobain Crystals) with a 3.0 mm inner diameter was employed, and samples were pressurized using helium gas; seven pressure points ranging from 1 to 120 bar (1, 20, 40, 60, 80, 100, and 120 bar) were obtained. Each sample was used for recording ^{15}N and ^{1}H CPMG dispersion measurements at two pressures, i.e., for no longer than 4 days. All data sets were measured at a single magnetic field strength of 14.1 T and at 25 °C on a Varian *Inova* spectrometer. ^{15}N (^{1}H) relaxation dispersion profiles were generated from peak intensities, $I_1(\nu_{CPMG})$, measured in a series of 17 (19) 2D ^{1}H−^{15}N correlation maps employing 14 (16) values of the CPMG field strength, ν_{CPMG}, ranging from 50 to 1000 (2000) Hz, with a constant relaxation time delay, T_{relax}, of 40 (30) ms (two duplicate points were recorded for error analysis). Peak intensities were extracted using the MUNIN approach (*23*, *24*) and were converted into effective relaxation rates using the relation $R_{2,eff} = -1/T_{relax}\ln[I_1(\nu_{CPMG})/I_0]$, where I_0 is the peak intensity in the reference spectrum obtained with a T_{relax} of 0. Uncertainties in $R_{2,eff}$ values were estimated as described previously (*20*).

The parameters of the three-site exchange model (F ↔ I ↔ U) were extracted by least-squares fits of calculated ($R_{2,\mathrm{eff}}^{\mathrm{clc}}$) to experimental ($R_{2,\mathrm{eff}}^{\mathrm{exp}}$) rates, measured in ^{1}H and ^{15}N single-quantum experiments as described elsewhere (*20*). Theoretical $R_{2,\mathrm{eff}}^{\mathrm{clc}}$ values were obtained by explicit numerical modeling of magnetization evolution during the CPMG sequence (*20*). The ^{1}H and ^{15}N SQ data for 44 residues of the G48M Fyn SH3 domain measured at the seven pressures were fit together assuming that the rate constants for interconversion between states (considered to be the same for all residues) follow pressure dependencies similar to eq 1

$$k_{\mathrm{i,j}} = (k_{\mathrm{B}}\kappa T/h)\exp[-\Delta G_{\mathrm{i-j}}/(RT)] \qquad (2)$$

where $\Delta G_{\mathrm{i-j}} = \Delta G_{0,\mathrm{i-j}} + \Delta V_{\mathrm{i-j}}(P - P_0)$, i, j ∈ {TS1, TS2, F, I, U}, and TS1 and TS2 denote transition states between U and I states and between I and F states, respectively. Thus, the differences in partial molar volumes between the exchanging states ($\Delta V_{\mathrm{i-j}}$) were extracted directly from the fit of relaxation dispersion data. It is notable that similar $\Delta V_{\mathrm{I-U}}$ and $\Delta V_{\mathrm{F-U}}$ values were obtained when dispersion data were fit directly, with the relation given by eq 2 enforced (as described above; method 1), or when rates were initially extracted from dispersion data without assuming any pressure dependence of exchange rates, with the rates extracted for different pressures subsequently fit to eq 2 to obtain volumes (method 2). It is also significant that there is little difference in the reduced χ^2 values that characterize the goodness of fit of the primary relaxation dispersion data using either approach (i.e., reduced $\chi^2 = 1.15$ and 1.12 for methods 1 and 2, respectively). However, method 1 was found to be more robust since it enforces a (very reasonable) pressure−rate constant dependence from the outset of the fitting procedure. We have also fit the dispersion profiles directly (i.e., method 1) to a simple model where $\Delta G_{\mathrm{i-j}} = \Delta G_{0,\mathrm{i-j}}$ (i.e., $\Delta V_{\mathrm{i-j}} = 0$) and to a more complex model where $\Delta G_{\mathrm{i-j}}$ is given by $\Delta G_{\mathrm{i-j}} = \Delta G_{0,\mathrm{i-j}} + \Delta V_{\mathrm{i-j}}(P - P_0) - 0.5\Delta\kappa_{\mathrm{T,i-j}}(P - P_0)^2$, where $\Delta\kappa_{\mathrm{T,i-j}}$ is the change in isothermal compressibility between states i and j. Reduced χ^2 values of 1.32 and 1.14 were obtained, respectively (relative to 1.15 when $\Delta\kappa_{\mathrm{T,i-j}} = 0$). In cases where the quadratic model of $\Delta G_{\mathrm{i-j}}(P)$ was used, however, large errors in the values of $\Delta V_{\mathrm{i-j}}$ and $\Delta\kappa_{\mathrm{i-j}}$ were obtained, with $\Delta\kappa_{\mathrm{i-j}}$ being a factor of 10 larger than expectations based on literature values. The large errors are not surprising. Assuming a value for $\Delta\kappa_{\mathrm{T,U-F}}$ of -18×10^{-6} mL g^{-1} bar^{-1} (*7*), the contribution that the quadratic term makes to $\Delta G_{\mathrm{i-j}}(P)$ is only 0.03 kcal/mol at a pressure of 120 bar, within the noise level; there is thus considerable "cross-talk" between $\Delta V_{\mathrm{i-j}}$ and $\Delta\kappa_{\mathrm{i-j}}$ in the fits. Dispersion data were therefore interpreted exclusively on the basis of a linear free energy pressure model. Finally, the uncertainties of the extracted model parameters (i.e., the values of intrinsic R_2 relaxation rates for 44 residues, k_{UI}, k_{IU}, k_{IF}, and k_{FI} at $P_0 = 1$ bar and $\Delta V_{\mathrm{TS1-U}}$, $\Delta V_{\mathrm{TS1-I}}$, $\Delta V_{\mathrm{TS2-I}}$, and $\Delta V_{\mathrm{TS2-F}}$) were estimated using the covariance matrix method (*25*). Figure 1B illustrates the positions of the 44 dynamics probes within the Fyn SH3 domain that have been used to extract volume changes accompanying the folding of this protein.

RESULTS AND DISCUSSION

Pressure Dependence of the Folding of the drkN SH3 Domain. At 15 °C and pH 6.0 and in aqueous buffer, the drkN SH3 domain exists in equilibrium between highly populated folded and unfolded states with a $\Delta G_{\mathrm{U-F}}$ close to 0 (*15*). We have previously shown that values of k_{f} and k_{u} differ by no more than 10% from site to site, establishing that to a good approximation the folding−unfolding reaction can be considered two-state (*16*). Under this set of conditions (15 °C, pH 6, and 1 bar), the folding and unfolding rates, k_{f} and k_{u}, respectively, are approximately 1.0 and 0.5 s^{-1}, respectively, so that exchange is slow on the NMR chemical shift time scale and separate peaks are thus observed for $\mathrm{F}_{\mathrm{exch}}$ and $\mathrm{U}_{\mathrm{exch}}$. A longitudinal nitrogen magnetization exchange experiment (*17*) can therefore be used to simultaneously obtain k_{f} and k_{u} under conditions that do not perturb the equilibrium. In this experiment, magnetization from each site is first labeled by the ^{15}N chemical shift, and subsequently, the exchange process between $\mathrm{F}_{\mathrm{exch}}$ and $\mathrm{U}_{\mathrm{exch}}$ states is monitored during a mixing period prior to the detection of the signal. In this way, correlations are observed at (ω_{Nf},ω_{Hf}) and (ω_{Nu},ω_{Hu}), corresponding to magnetization that is not transferred between states during the mixing time (auto-peaks, denoted by ff and uu, respectively, for Ala 3 in the inset of Figure 2A) and at (ω_{Nf},ω_{Hu}) and (ω_{Nu},ω_{Hf}) (cross-peaks, denoted by fu and uf, respectively) in the case where transfer from $\mathrm{F}_{\mathrm{exch}}$ to $\mathrm{U}_{\mathrm{exch}}$ or from $\mathrm{U}_{\mathrm{exch}}$ to $\mathrm{F}_{\mathrm{exch}}$ occurs. In principle, each amide site in the protein contributes the four peaks described above, as illustrated in Figure 2A; however, in practice, a complete set of four correlations is observed for a relatively small number of residues due to overlap (nine residues were selected in this study). The mixing time dependencies of the volumes of the auto-peaks and cross-peaks, shown in Figure 2A, are globally fit to extract k_{f} and k_{u}, as described in Materials and Methods. The nitrogen magnetization decay−exchange profiles illustrated in Figure 2A have been recorded as a function of pressure, ranging from 1 to 75 bar, with the corresponding changes in the exchange profiles for Ala 3 illustrated in Figure 2B for the extreme pressure points. The sensitivity of the methodology to small changes in rates with pressure becomes apparent when one considers that the k_{f} value decreases from 1.11 to 0.86 s^{-1} when the pressure is increased from 1 to 75 bar, yet substantial differences in the buildup profiles corresponding to the exchange of magnetization from $\mathrm{U}_{\mathrm{exch}}$ to $\mathrm{F}_{\mathrm{exch}}$ are observed (compare solid and dashed green lines in Figure 2B). Of note, the unfolding rate is much less affected by pressure than the folding rate, consistent with the relation $|\Delta V_{\mathrm{F-TS}}| < |\Delta V_{\mathrm{U-TS}}|$ (see eq 1 and below).

Figure 2C shows the pressure dependencies of the free energy differences $\Delta G_{\mathrm{TS-U}}$ (empty squares), $\Delta G_{\mathrm{TS-F}}$ (empty triangles), and $\Delta G_{\mathrm{U-F}}$ (filled squares) obtained from $k_{\mathrm{f}}(P)$, $k_{\mathrm{u}}(P)$, and $k_{\mathrm{u}}(P)/k_{\mathrm{f}}(P)$, respectively, along with the best fits to the experimental data (solid lines) using the relation $\Delta G_{\mathrm{i-j}} = \Delta G_{0,\mathrm{i-j}} + \Delta V_{\mathrm{i-j}}(P - P_0)$. A plot of $\Delta V = (\partial\Delta G/\partial P)_T$ along the folding reaction coordinate is shown in Figure 2D. The volume of the protein−solvent system in the folded state, $\mathrm{F}_{\mathrm{exch}}$, is higher than that in the unfolded state, $\mathrm{U}_{\mathrm{exch}}$ ($\Delta V_{\mathrm{F-U}} = 74 \pm 4$ mL/mol), while the volume of the transition state ensemble (TSE) is significantly greater than the volume of the U ensemble and somewhat greater than the volume of

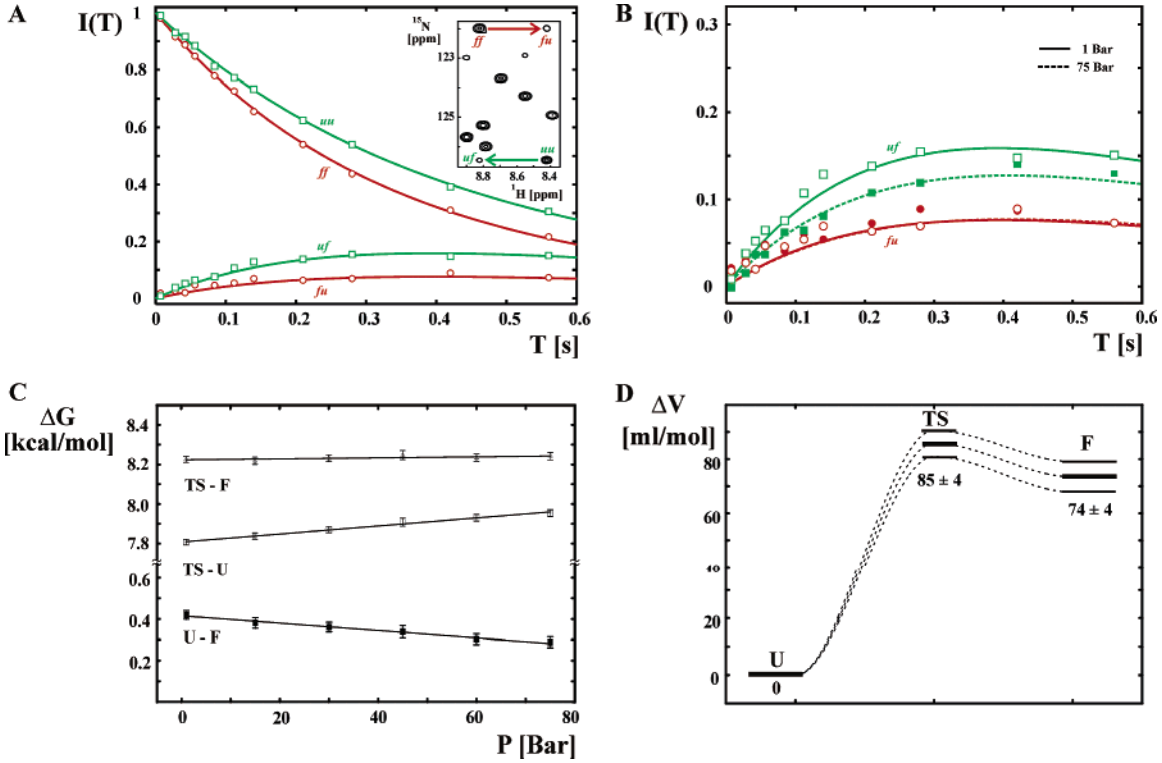

FIGURE 2: Pressure-dependent folding of the drkN SH3 domain. (A) Time dependence of the decay of auto-peaks (ff and uu) and buildup of exchange cross-peaks (fu and uf) corresponding to the evolution of nitrogen longitudinal magnetization during a mixing time, *T*. The data for Ala 3, at 15 °C and 1 bar, are shown (the portion of the $^{1}H-^{15}N$ correlation spectrum from which the exchange data is obtained is presented as an inset). Empty circles (red lines) show experimental peak integrals (best fit curves) for the ff and fu correlations corresponding to magnetization originating in the folded state, while empty squares (green lines) denote peak integrals (best fit curves) for the uu and uf peaks, derived from magnetization originating in the unfolded state. The volumes of ff and uu correlations at zero mixing time were normalized to 1; the volumes of all correlations were corrected for relaxation during the pulse scheme (*16*). (B) Pressure dependencies of the uf and fu exchange cross-peaks shown in panel A. Empty and filled symbols correspond to data obtained at pressures of 1 and 75 bar, respectively; other symbols are defined as described above. (C) Pressure dependencies of the free energy differences ΔG_{TS-U} (empty squares), ΔG_{TS-F} (triangles), and ΔG_{U-F} (filled squares), derived from the folding rate, k_f, the unfolding rate, k_u, and the equilibrium constant, k_u/k_f, respectively. The best fit lines are solid lines, corresponding to the following values: $k_u = 0.54 \pm 0.01\ s^{-1}$, $k_f = 1.11 \pm 0.01\ s^{-1}$, and $k_u/k_f = 0.49 \pm 0.01$. (D) Partial molar volume of the drkN SH3 solvent system as a function of folding, referenced to the volume of the unfolded state (the central line denotes best fit values, with outer lines enclosing values within one standard deviation).

the folded state ($\Delta V_{TS-U} = 85 \pm 4$ mL/mol). The few kinetic studies of protein folding and unfolding with pressure that have been reported to date have also focused on systems that fold by a two-state mechanism. As observed for the drkN SH3 domain, the activation volumes for folding and unfolding reported in these studies usually place the transition state closer to the folded state along the folding coordinate (*13*, *31*−*33*).

Pressure Dependence of the Folding of the G48M Fyn SH3 Domain. In a recent study, we have shown that the millisecond time scale folding−unfolding reaction for the [^{2}H,^{15}N]G48M Fyn SH3 domain can be described by a three-state model (F ↔ I ↔ U) where states I and U are populated at approximately 1 and 5%, respectively, at 25 °C and 1 bar (*20*). The rate parameters and populations that characterize the folding reaction under these conditions have been extracted using a suite of six CPMG-based relaxation dispersion experiments recorded at each of three magnetic field strengths. Repeating this complete set of experiments for each of the seven pressures reported here (ranging from 1 to 120 bar) would be time-consuming, and sample stability would become an issue. Therefore, we use a pair of experiments to generate ^{15}N and ^{1}H single-quantum dispersion profiles, at 25 °C, as a function of pressure. Dispersion profiles for 44 amide groups measured at all pressures are subsequently fit together, enforcing the rate constant pressure dependencies given by eq 2 and fixing the chemical shift differences between states to the values obtained previously from an analysis of the suite of six experiments recorded at three fields on a sample of the [^{2}H,^{15}N]G48M Fyn SH3 domain at 1 bar (*20*). It is worth mentioning that fitting all of the pressure data together (see Materials and Methods) leads to a significant sensitivity improvement relative to an analysis in which data at each pressure point are examined independently, compensating to some extent for the fact that only a pair of dispersion profiles were recorded.

Figure 3A shows ^{15}N (green) and ^{1}H (red) single-quantum relaxation dispersion profiles measured for a pair of the 44 residues used in the analysis, His 21 (filled symbols) and Asp 9 (empty symbols) of [^{2}H,^{15}N]G48M Fyn SH3 at 25 °C, 1 bar, and 14.1 T, with the corresponding region of the $^{1}H-^{15}N$ correlation spectrum shown as an inset. The pressure dependence of the ^{15}N and ^{1}H dispersion profiles for Asp 9 is shown in Figure 3B (colored green and red, respectively). Although the effects are quite subtle, in general $R_{2,eff}$(50 Hz) − $R_{2,eff}$(1000 Hz) increases with pressure (see in particular the ^{1}H dispersion profile), mainly reflecting growth in the population of the unfolded state (see below). The pressure dependencies of the free energy differences, ΔG_{TS1-U}, ΔG_{TS1-I}, ΔG_{TS2-I}, and ΔG_{TS2-F}, as well as differences ΔG_{U-F}

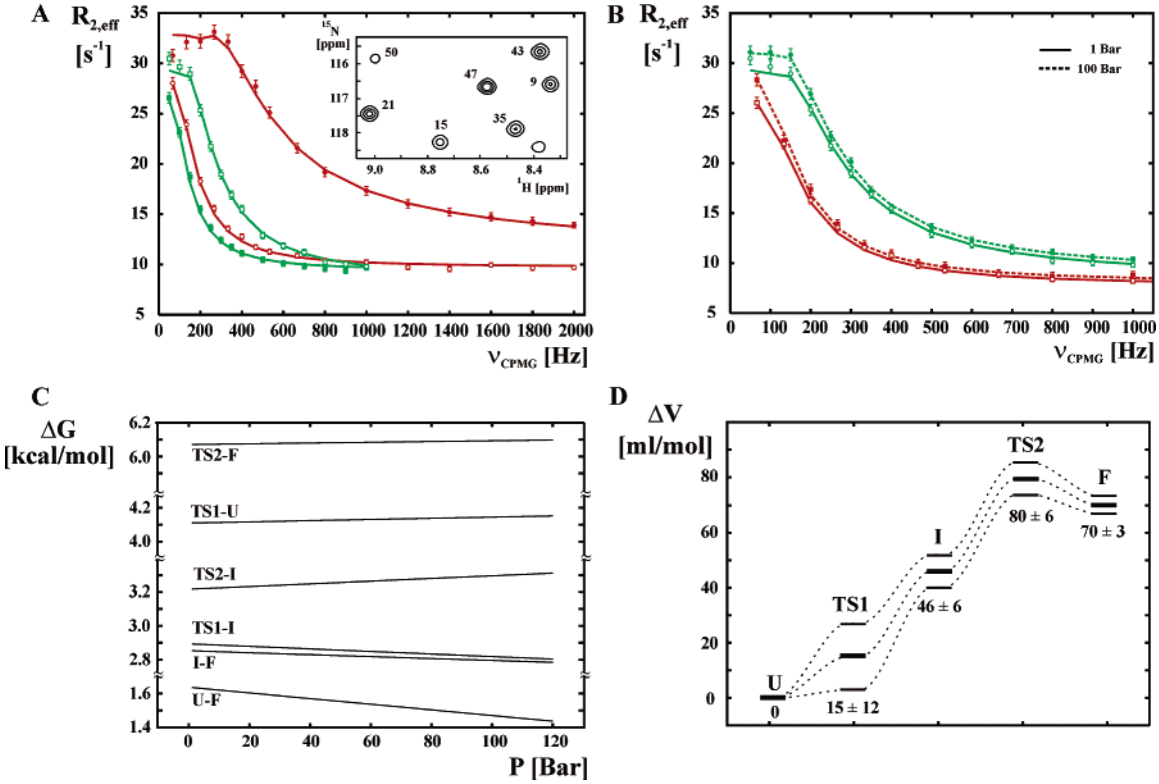

FIGURE 3: Pressure-dependent folding of the G48M Fyn SH3 domain. (A) ^{1}H (circles, red lines) and ^{15}N (squares, green lines) single-quantum CPMG dispersion profiles of Asp 9 (empty symbols) and His 21 (filled symbols) as a function of CPMG frequency, ν_{CPMG}, measured at 1 bar, with the corresponding region of the ^{1}H−^{15}N correlation spectrum shown as an inset. (B) Pressure dependence of ^{1}H (red) and ^{15}N (green) dispersion profiles for Asp 9. Empty symbols (solid lines) denote the data (best fits) obtained at 1 bar, whereas filled symbols (dashed lines) correspond to the data (best fit curves) at 100 bar. For clarity of presentation, 2 s^{-1} was subtracted from the ^{1}H dispersion profiles. The following values were obtained from global fits of the data, as described in the text: $p_I = 0.75 \pm 0.01\%$, $p_U = 5.88 \pm 0.04\%$, $k_{FI} + k_{IF} = 4310 \pm 78$ s^{-1}, and $k_{IU} + k_{UI} = 8359 \pm 326$ s^{-1} at 1 bar. (C) Pressure dependencies of the free energy differences ΔG_{i-j} (denoted i−j) calculated from values of the fitting parameters, $\Delta G_{0,i-j}$ and ΔV_{i-j}. To improve the accuracy of the extracted ΔV values, dispersion data at all pressures were fit together, omitting the intermediate step where rates (or free energies) as a function of pressure are obtained. To emphasize this, we have chosen not to highlight the ΔG values for the seven experimental values of pressure used in the analysis. (D) Partial molar volume of the G48M Fyn SH3 solvent system (see Figure 2 for an additional description).

and ΔG_{I-F} (where $\Delta G_{i-j} = G_i - G_j$), extracted from fits of the dispersion data are illustrated in Figure 3C, with the corresponding changes in ΔV indicated in Figure 3D. As in the case of the drkN SH3 domain, the volume of the G48M Fyn SH3 domain in the folded state F is greater than that in the unfolded state U ($\Delta V_{F-U} = 70 \pm 3$ mL/mol). Approximately 65% of the volume change upon folding occurs during the transition from U to I ($\Delta V_{I-U} = 46 \pm 6$ mL/mol), with the volume of TS1 between U and I very close to the volume of U ($\Delta V_{TS1-U} = 15 \pm 12$ mL/mol). TS2, between states I and F, has the greatest volume along the folding trajectory ($\Delta V_{TS2-U} = 80 \pm 6$ mL/mol), similar to what is observed for the transition state TS between the U_{exch} and F_{exch} states of the drkN SH3 domain.

Relating Volume Changes along the Folding Pathway to Hydration and Packing. The partial molar volume differences (ΔV_{U-F}) that have been measured between the U and F states of the drkN and G48M Fyn SH3 domains, -74 ± 5 and -70 ± 3 mL/mol, respectively, are consistent with the results of numerous volumetric studies of small- and medium-sized proteins (*6*, *34*). The very slightly different values of ΔV_{U-F} obtained for the two SH3 domains that are similar in size may be due to the different temperatures that are used (i.e., 15 °C for drkN SH3 and 25 °C for G48M Fyn SH3) and the positive change of partial molar expansibility $\Delta\epsilon = (\partial\Delta V/\partial T)_P$ upon unfolding (*6*), or to other differences in experimental conditions such as pH.

The origin of the volume changes that accompany protein folding−unfolding transitions has been the subject of an ongoing discussion in the literature. The complexity arises, in no small part, because measured values of ΔV_{U-F} are the result of an interplay between a number of compensating factors. These include (i) an increasing degree of hydration of the newly exposed charged and polar groups upon unfolding, leading to a decrease in the overall volume of the protein−water system that reflects the higher density of the water in the protein solvent shell relative to bulk water (*6*, *35*, *36*), (ii) the elimination of internal voids in the folded protein that also leads to negative contributions to ΔV_{U-F} (*6*, *35*, *36*), (iii) an increase in ΔV_{U-F} reflecting the fact that most atoms on a protein surface occupy a larger volume than in the core (*37*), and (iv) increases in the void volume around the solute that increases ΔV_{U-F} (*35*). Chalikian and Breslauer describe the latter effect as being proportional to the difference in solvent accessible surface areas between U and F states and resulting from mutual vibrations between contacting solvent and solute molecules (*35*). The balance between these terms is such that they effectively offset each other so that the net change in ΔV_{U-F} is only 1−2% of the partial molar volume of either the U or F state (*34*). Thus,

although the data from Figures 2 and 3 establish that ΔV can be obtained from pressure-dependent studies of protein folding kinetics as monitored by NMR spectroscopy, interpretation of the data in molecular terms must be made cautiously. Fortunately, a significant body of related information is available on the folding of SH3 domains in general and for the pair of proteins considered here, in particular, to guide interpretation of the volumetric data.

The partial molar volume profile along the folding pathway of the drkN SH3 domain (Figure 2D) allows several qualitative statements to be made regarding the nature of the TSE. In particular, the increase in volume of the TSE relative to the unfolded state is consistent with the collapse of the unfolded polypeptide chain to a loosely packed structure; packing defects in such a loose structure would then account for the large and positive ΔV_{TS-U} value. Such a picture is consistent with a large body of data from protein engineering-based ϕ value analysis of SH3 domains, interpreted on the basis of a two-state folding model, that suggests that the TSEs in these proteins are reasonably well packed at a small number of key residues, with less constrained structure at other positions (*38*, *39*). The small value for ΔV_{TS-F} could well be the result of two competing terms corresponding to (i) an increase in the intrinsic volume of the TSE relative to F_{exch} due to a greater number of packing defects in the TSE and (ii) a decrease in the protein−water volume from contraction of solvent in the vicinity of polar and charged residues that are more accessible in the TSE than in the F_{exch} state. In this model, the TSE would be at least partially hydrated, consistent with a number of simulation studies that have been reported for SH3 domain folding (*40*, *41*). The pressure-derived insights into the volume of the transition state are complementary to urea and glycerol folding kinetic studies indicating that 25% of the surface area exposed upon unfolding is accessible in the TSE, which is at least partially hydrated (M. Tollinger et al., manuscript in preparation).

The folding of the G48M mutant Fyn SH3 domain has been modeled by a three-state mechanism so that the partial molar volume profile can be sampled more extensively than that for the drkN SH3 domain (compare Figures 2D and 3D). Insight into some of the structural and thermodynamic properties of each of the states along the folding coordinate has been obtained in a series of previous studies at a pressure of 1 bar. ^{15}N and ^{1}H chemical shift differences among F, I, and U states suggest that β-strands $\beta2-\beta4$ (Figure 1B) of the I state are at least partially formed (*19*, *20*), although random coil like methyl ^{13}C chemical shifts for the I state argue against the formation of specific interactions between hydrophobic side chains (*27*). Additional experiments, where folding rates were obtained for fully protonated, partially deuterated, and fully deuterated proteins, led to the conclusion that some van der Waals (VDW) interactions were formed in each of the TS1, I, and TS2 states, suggesting at least partially collapsed structures (*27*). The volumetric measurements reported in this work are consistent with and complement previous work, providing a more comprehensive view of changes in chain hydration and packing upon Fyn SH3 domain folding. The progressive increase in volume from U to TS1 to I, along with kinetic studies as a function of deuteration that were reported previously (*27*) (see above), suggests that TS1 is largely unstructured, not unlike the U state, but with some VDW interactions formed. The I state ensemble would be more collapsed (albeit with many packing defects) and, on the basis of previous chemical shift results, likely involves (partial) formation of the central β-sheet, comprised of strands 2−4 (Figure 1B). The volume data reported here (ΔV_{TS1-U}, $\Delta V_{I-U} < \Delta V_{F-U}$) are consistent with a higher level of hydration for TS1 and I relative to F.

Molecular dynamics simulations of the folding of the src-SH3 domain also show two barriers (i.e., three-state folding) with TS2 comprised of two preformed hydrophobic surfaces, one involving strands $\beta2-\beta4$ and the other $\beta1$, $\beta5$, and the RT-src loop (*40*, *41*). The transition from I to F would then involve reorganization of these surfaces to form the native side chain packing configuration of the F state, with concomitant release of water from the tightly formed hydrophobic interface. The large increase in ΔV observed here between I and F is consistent with dehydration at some point along this portion of the pathway.

It is tempting to speculate that the TS of the drkN SH3 domain is similar to TS2 of G48M Fyn SH3. Note that TS and TS2 have the largest volumes along their respective folding pathways, with ΔV_{TS-F} and ΔV_{TS2-F} being ~10 mL/mol. Although the folding process monitored for the drkN SH3 domain is fit well to a two-state model, a large body of data collected on this domain provides evidence of an initial structural collapse within the ensemble of the unfolded state, U_{exch} (*42*−*44*), much like TS1 and I of the Fyn SH3 domain (whose NMR folding data can be well fit to only a three-state model). For example, hydrodynamic studies, including small-angle X-ray scattering and pulsed field gradient NMR experiments, have established that the U_{exch} ensemble is only approximately 40% larger than that of the F_{exch} state, significantly more compact than the guanidinium unfolded state that is 85% larger than F_{exch} (*45*). In addition, backbone and side chain NOEs (*42*, *43*), spin relaxation experiments (*46*), and fluorescence measurements indicate the formation of both native- and non-native-like structural elements within the U_{exch} ensemble (*44*). Long-range NOEs suggest the presence of native-like interactions between residues in the central β-sheet, particularly between strands $\beta5$ and $\beta6$ of the drkN SH3 domain (corresponding to $\beta3$ and $\beta4$, respectively, in Fyn SH3) (Figure 1) (*42*), while non-native contacts involve hydrophobic clustering around the Trp 36 indole and formation of transient α-helical structure in the region including residues Ser 18−Ile 24 (*43*, *47*). Further evidence for the existence of several substates within the U_{exch} ensemble is provided by ^{15}N CPMG dispersion experiments that show millisecond time scale conformational exchange in the U_{exch} state involving residues Leu 25−Leu 28 (*16*).

CONCLUDING REMARKS

In this work, we have used NMR spin relaxation techniques to measure the folding−unfolding kinetics of a pair of SH3 domains that fold with rates differing by ~3 orders of magnitude. The NMR methodology used is sensitive to even small changes in rate constants so that reliable changes in partial molar volume along the folding trajectories of both proteins can be obtained using relatively low pressures (1−120 bar). This helps minimize any significant pressure-induced perturbations to the more "delicate" structures (U,

I, and TSE) that are formed during the folding process. Despite the small pressure effects on folding, the different models used to fit the data (i.e., two- vs three-state) and the different folding time scales, the partial molar volume profiles for both proteins display distinct similarities, as might be expected. This provides confidence in both the primary relaxation data and the analysis procedures that were employed. The volume profiles have been interpreted in terms of changes in protein hydration and packing accompanying folding and are consistent with a model of initial collapse and formation of a partially compact structure that is at least somewhat hydrated. This study makes it clear that NMR relaxation methods are a powerful complement to the more traditional approaches for measuring volumetric properties associated with protein folding reactions where perturbants such as extremes of pH, denaturants, or high pressures are often employed.

ACKNOWLEDGMENT

We are grateful to Professors T. Chalikian (University of Toronto) and H. S. Chan (University of Toronto) for valuable discussions.

SUPPORTING INFORMATION AVAILABLE

Description of the protocol used for measuring volumes of correlations in 2D ^{15}N magnetization exchange spectra. This material is available free of charge via the Internet at http://pubs.acs.org.

REFERENCES

1. Fersht, A. (1999) *Structure and Mechanism in Protein Science*, W. H. Freeman and Co., New York.
2. Dinner, A. R., Sali, A., Smith, L. J., Dobson, C. M., and Karplus, M. (2000) Understanding protein folding via free-energy surfaces from theory and experiment, *Trends Biochem. Sci. 25*, 331−9.
3. Dyson, H. J., and Wright, P. E. (2002) Insights into the structure and dynamics of unfolded proteins from nuclear magnetic resonance, *Adv. Protein Chem. 62*, 311−40.
4. Shortle, D. (1996) Structural analysis of non-native states of proteins by NMR methods, *Curr. Opin. Struct. Biol. 6*, 24−30.
5. Plaxco, K. W., and Baker, D. (1998) Limited internal friction in the rate-limiting step of a two-state protein folding reaction, *Proc. Natl. Acad. Sci. U.S.A. 95*, 13591−6.
6. Chalikian, T. V. (2003) Volumetric properties of proteins, *Annu. Rev. Biophys. Biomol. Struct. 32*, 207−35.
7. Taulier, N., and Chalikian, T. V. (2002) Compressibility of protein transitions, *Biochim. Biophys. Acta 1595*, 48−70.
8. Silva, J. L., and Weber, G. (1993) Pressure stability of proteins, *Annu. Rev. Phys. Chem. 44*, 89−113.
9. Sarvazyan, A. P. (1991) Ultrasonic velocimetry of biological compounds, *Annu. Rev. Biophys. Biophys. Chem. 20*, 321−42.
10. Prehoda, K. E., Mooberry, E. S., and Markley, J. L. (1998) Pressure denaturation of proteins: Evaluation of compressibility effects, *Biochemistry 37*, 5785−90.
11. Fuentes, E. J., and Wand, A. J. (1998) Local stability and dynamics of apocytochrome b_{562} examined by the dependence of hydrogen exchange on hydrostatic pressure, *Biochemistry 37*, 9877−83.
12. Akasaka, K. (2003) Highly fluctuating protein structures revealed by variable-pressure nuclear magnetic resonance, *Biochemistry 42*, 10875−85.
13. Pappenberger, G., Saudan, C., Becker, M., Merbach, A. E., and Kiefhaber, T. (2000) Denaturant-induced movement of the transition state of protein folding revealed by high-pressure stopped-flow measurements, *Proc. Natl. Acad. Sci. U.S.A. 97*, 17−22.
14. Taulier, N., Beletskaya, I. V., and Chalikian, T. V. (2005) Compressibility changes accompanying conformational transitions of apomyoglobin, *Biopolymers 79*, 218−29.
15. Zhang, O., and Forman-Kay, J. D. (1995) Structural characterization of folded and unfolded states of an SH3 domain in equilibrium in aqueous buffer, *Biochemistry 34*, 6784−94.
16. Tollinger, M., Skrynnikov, N. R., Mulder, F. A. A., Forman-Kay, J. D., and Kay, L. E. (2001) Slow dynamics in folded and unfolded states of an SH3 domain, *J. Am. Chem. Soc. 123*, 11341−52.
17. Farrow, N. A., Zhang, O., Forman-Kay, J. D., and Kay, L. E. (1994) A heteronuclear correlation experiment for simultaneous determination of ^{15}N longitudinal decay and chemical exchange rates of systems in slow equilibrium, *J. Biomol. NMR 4*, 727−34.
18. Tollinger, M., Kay, L. E., and Forman-Kay, J. D. (2005) Measuring pK_a values in protein folding transition state ensembles by NMR spectroscopy, *J. Am. Chem. Soc. 127*, 8904−5.
19. Korzhnev, D. M., Salvatella, X., Vendruscolo, M., Di Nardo, A. A., Davidson, A. R., Dobson, C. M., and Kay, L. E. (2004) Low-populated folding intermediates of Fyn SH3 characterized by relaxation dispersion NMR, *Nature 430*, 586−90.
20. Korzhnev, D. M., Neudecker, P., Mittermaier, A., Orekhov, V. Y., and Kay, L. E. (2005) Multiple-Site Exchange in Proteins Studied with a Suite of Six NMR Relaxation Dispersion Experiments: An Application to the Folding of a Fyn SH3 Domain Mutant, *J. Am. Chem. Soc. 127*, 15602−11.
21. Palmer, A. G., Kroenke, C. D., and Loria, J. P. (2001) NMR methods for quantifying microsecond-to-millisecond motions in biological macromolecules, *Methods Enzymol. 339*, 204−38.
22. Bezsonova, I., Singer, A., Choy, W. Y., Tollinger, M., and Forman-Kay, J. D. (2005) Structural comparison of the unstable drkN SH3 domain and a stable mutant, *Biochemistry 44*, 15550−60.
23. Korzhnev, D. M., Ibraghimov, I. V., Billeter, M., and Orekhov, V. Y. (2001) MUNIN: Application of three-way decomposition to the analysis of heteronuclear NMR relaxation data, *J. Biomol. NMR 21*, 263−8.
24. Orekhov, V. Y., Ibraghimov, I. V., and Billeter, M. (2001) MUNIN: A new approach to multi-dimensional NMR spectra interpretation, *J. Biomol. NMR 20*, 49−60.
25. Press, W. H., Flannery, B. P., Teukolsky, S. A., and Vetterling, W. T. (1988) *Numerical Recipes in C*, Cambridge University Press, Cambridge, U.K.
26. Hagen, S. J., Hofrichter, J., Szabo, A., and Eaton, W. A. (1996) Diffusion-limited contact formation in unfolded cytochrome *c*: Estimating the maximum rate of protein folding, *Proc. Natl. Acad. Sci. U.S.A. 93*, 11615−7.
27. Mittermaier, A., Korzhnev, D. M., and Kay, L. E. (2005) Side-chain interactions in the folding pathway of a Fyn SH3 domain mutant studied by relaxation dispersion NMR spectroscopy, *Biochemistry 44*, 15430−6.
28. Korzhnev, D. M., Bezsonova, I., Evanics, F., Taulier, N., Zhou, Z., Bai, Y., Chalikian, T. V., Prosser, R. S., and Kay, L. E. (2006) Probing the transition state ensemble of a protein folding reaction by pressure dependent NMR relaxation dispersion, *J. Am. Chem. Soc.* (in press).
29. Loria, J. P., Rance, M., and Palmer, A. G. (1999) A relaxation compensated CPMG sequence for characterizing chemical exchange, *J. Am. Chem. Soc. 121*, 2331−2.
30. Ishima, R., and Torchia, D. (2003) Extending the range of amide proton relaxation dispersion experiments in proteins using a constant-time relaxation-compensated CPMG approach, *J. Biomol. NMR 25*, 243−8.
31. Jacob, M. H., Saudan, C., Holtermann, G., Martin, A., Perl, D., Merbach, A. E., and Schmid, F. X. (2002) Water contributes actively to the rapid crossing of a protein unfolding barrier, *J. Mol. Biol. 318*, 837−45.
32. Vidugiris, G. J., Markley, J. L., and Royer, C. A. (1995) Evidence for a molten globule-like transition state in protein folding from determination of activation volumes, *Biochemistry 34*, 4909−12.
33. Woenckhaus, J., Kohling, R., Thiyagarajan, P., Littrell, K. C., Seifert, S., Royer, C. A., and Winter, R. (2001) Pressure-jump small-angle X-ray scattering detected kinetics of staphylococcal nuclease folding, *Biophys. J. 80*, 1518−23.
34. Chalikian, T. V., and Filfil, R. (2003) How large are the volume changes accompanying protein transitions and binding? *Biophys. Chem. 104*, 489−99.
35. Chalikian, T. V., and Bresiauer, K. J. (1996) On volume changes accompanying conformational transitions of biopolymers, *Biopolymers 39*, 619−26.

36. Silva, J. L., Foguel, D., and Royer, C. A. (2001) Pressure provides new insights into protein folding, dynamics and structure, *Trends Biochem. Sci. 26*, 612−8.
37. Gerstein, M., Tsai, J., and Levitt, M. (1995) The volume of atoms on the protein surface: Calculated from simulation, using Voronoi polyhedra, *J. Mol. Biol. 249*, 955−66.
38. Northey, J. G. B., Di Nardo, A. A., and Davidson, A. R. (2002) Hydrophobic core packing in the SH3 domain folding transition state, *Nat. Struct. Biol. 9*, 126−30.
39. Plaxco, K. W., Guijarro, J. I., Morton, C. J., Pitkeuthly, M., Campbell, I., and Dobson, C. M. (1998) The folding kinetics and thermodynamics of the Fyn-SH3 domain, *Biochemistry 37*, 2529−37.
40. Shea, J. E., Onuchic, J. N., and Brooks, C. L., III (2002) Probing the folding free energy landscape of the Src-SH3 protein domain, *Proc. Natl. Acad. Sci. U.S.A. 99*, 16064−8.
41. Guo, W., Lampoudi, S., and Shea, J. E. (2003) Posttransition state desolvation of the hydrophobic core of the src-SH3 protein domain, *Biophys. J. 85*, 61−9.
42. Mok, Y. K., Kay, C. M., Kay, L. E., and Forman-Kay, J. D. (1999) NOE data demonstrating a compact unfolded state for an SH3 domain under non-denaturing conditions, *J. Mol. Biol. 289*, 619−38.
43. Crowhurst, K. A., and Forman-Kay, J. D. (2003) Aromatic and methyl NOEs highlight hydrophobic clustering in the unfolded state of an SH3 domain, *Biochemistry 42*, 8687−95.
44. Crowhurst, K. A., Tollinger, M., and Forman-Kay, J. D. (2002) Cooperative interactions and a non-native buried Trp in the unfolded state of an SH3 domain, *J. Mol. Biol. 322*, 163−78.
45. Choy, W. Y., and Forman-Kay, J. D. (2001) Calculation of ensembles of structures representing the unfolded state of an SH3 domain, *J. Mol. Biol. 308*, 1011−32.
46. Yang, D., Mok, Y. K., Muhandiram, D. R., Forman-Kay, J. D., and Kay, L. E. (1999) $^{1}H-^{13}C$ dipole−dipole cross-correlated spin relaxation as a probe of dynamics in unfolded proteins: Application to the drkN SH3 domain, *J. Am. Chem. Soc. 121*, 3555−6.
47. Mok, Y. K., Elisseeva, E. L., Davidson, A. R., and Forman-Kay, J. D. (2001) Dramatic stabilization of an SH3 domain by a single substitution: Roles of the folded and unfolded states, *J. Mol. Biol. 307*, 913−28.
48. Noble, M. E., Musacchio, A., Saraste, M., Courtneidge, S. A., and Wierenga, R. K. (1993) Crystal structure of the SH3 domain in human Fyn: Comparison of the three-dimensional structures of SH3 domains in tyrosine kinases and spectrin, *EMBO J. 12*, 2617−24.

BI060177R